Electronic Supplementary Material (ESI) for Journal of Materials Chemistry

Indole-substituted nickel dithiolene complexes in electronic and optoelectronic devices

Simon Dalgleish, John G. Labram, Zhe Li, Jianpu Wang, Christopher R. McNeill, Thomas Anthopolous, Neil C. Greenham and Neil Robertson

Supplementary Information

Bond	Bond Length / Å			
	Complex **4**		Complex **3**	Pro-ligand **1**
	Observed	Calculated	Calculated	Observed
Ni(1)-S(2)	2.1260(8)	2.124090	2.126509	-
Ni(1)-S(9)	2.1217(8)	2.123360	2.126562	-
S(2)-C(3)	1.707(3)	1.718131	1.699005	1.737(5)
S(9)-C(8)	1.714(3)	1.725658	1.728363	1.746(5)
C(3)-C(8)	1.377(5)	1.391029	1.384233	1.336(7)
Angle	Angle Size / ^{o}			
	Observed	Calculated	Calculated	Observed
S(2)-C-C-S(9)	0.28	0.02	0.8	0.43
C-C-C-C	59.89	53.93	30.14	30.96

*Table S1: (upper) Selected bond lengths of **3** and **4**, showing a good general agreement of calculated bond lengths with those observed for single crystal XRD data of **4**, and a reduction in the C-S bond lengths and increase in the C=C bond lengths, compared to that of the single crystal XRD data of pro-ligand **2**, confirming the aromatic nature of the NiSCCS ring. (lower) Selected torsion angles of **3** and **4** showing an overall square planar coordination geometry with the pendent indolyl groups twisted away from planarity.*

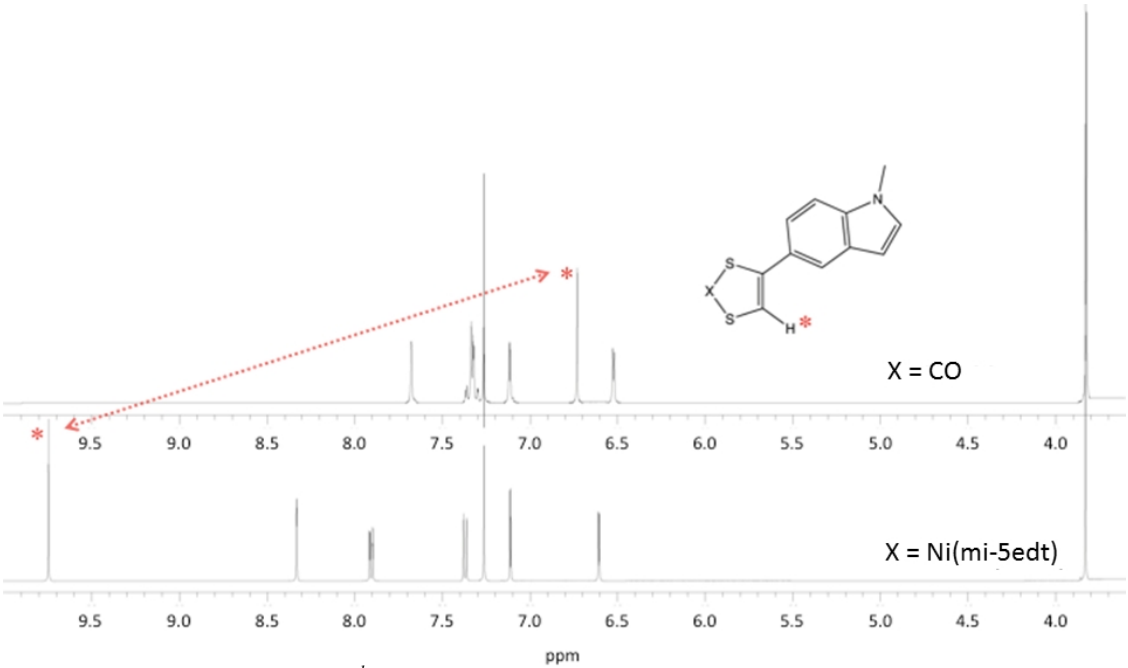

*Figure S1: An expansion of the ^{1}H NMR spectra of **1** and **3**, showing the increased aromaticity of the dithiolene upon complexation by the large shift to higher frequency for the ethylene proton (*).*

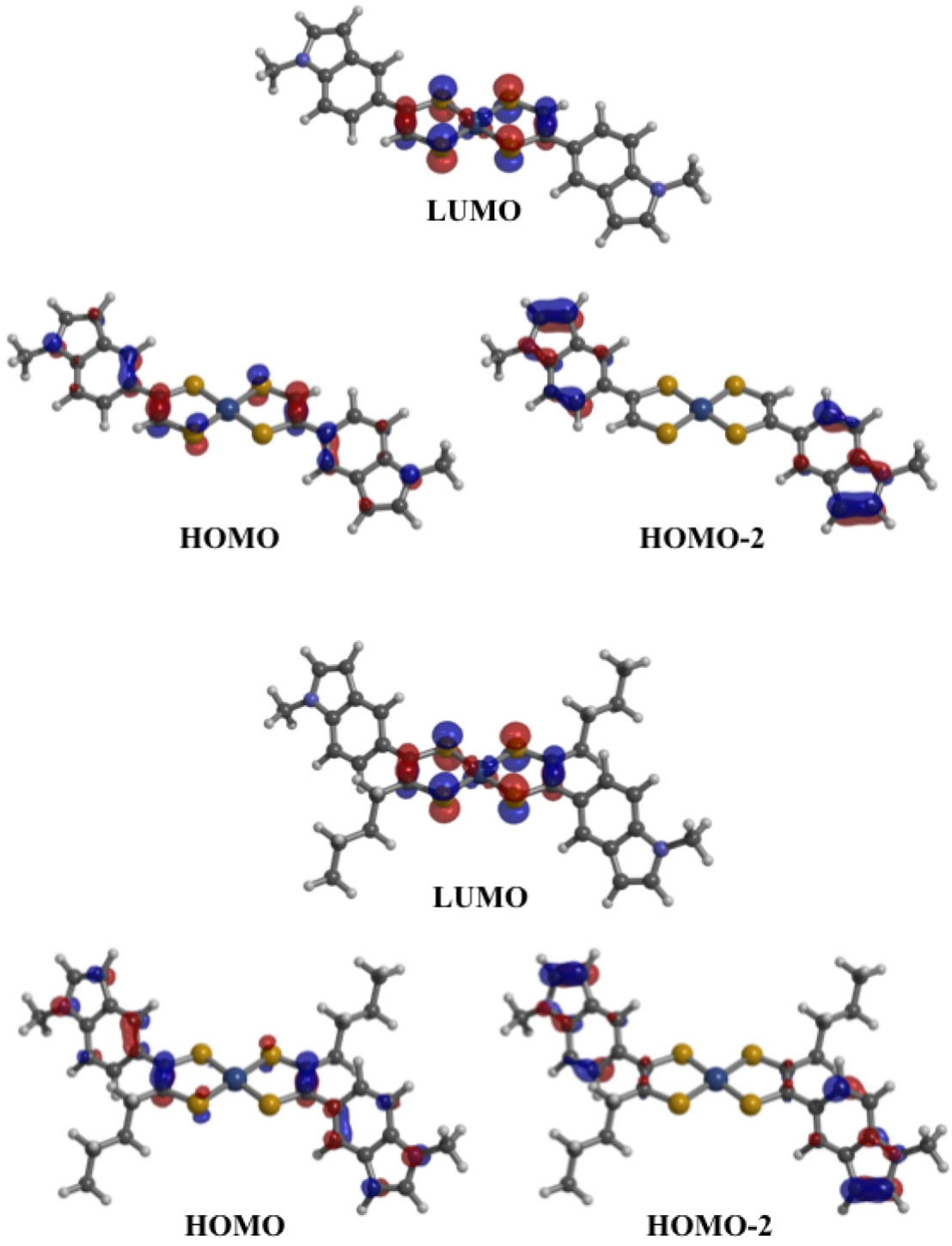

Figure S2: Frontier molecular orbitals of ***3*** *(upper) and* ***4*** *(lower) that contribute to the low energy absorption in the NIR region, calculated from the geometry optimised structures, with starting geometry based on single crystal X-ray data obtained for* ***4****.*

Complex	Wavelength / nm	Osc. strength	Major contributions
3	921.1	0.3164	HOMO→LUMO (57 %) HOMO-2→LUMO (22 %)
	786.5	0.2828	HOMO-2→LUMO (73 %) HOMO→LUMO (10 %)
4	899.7	0.2955	HOMO→LUMO (70 %) HOMO-2→LUMO (14 %)
	747.0	0.1789	HOMO-2→LUMO (78 %) HOMO→LUMO (4 %)

Complex	Orbital	Orbital location %	
		Ni	Ligand (SCCS)
3	LUMO	17.13	82.87 (72.71)
	HOMO	1.44	98.56 (50.17)
	HOMO-2	0.48	99.52 (9.75)
4	LUMO	17.83	82.17 (72.53)
	HOMO	1.69	98.31 (46.22)
	HOMO-2	0.69	99.31 (19.75)

*Table S2: TD-DFT data: calculated energies and intensities of the transition observed in **3** and **4**; calculated contributions to the frontier molecular orbitals contributing to the NIR absorption of **3** and **4**. The data confirm the low energy absorption to be due to transitions between orbitals delocalised over the dithiolene core, with substantial contribution from the indolyl groups. The large oscillator strength is consistent with the high degree of spatial overlap of the frontier orbitals.*

Complex	$E^1_{1/2}$ / V	$E^2_{1/2}$ / V	E^3_{ox} / V	E^4_{ox} / V
3	-0.76	0.07	0.92*	1.46*
4	-0.90	-0.03	1.12	1.46*

*Table S3: Redox levels of **3** and **4** (vs. Ag/AgCl) in 0.3 M $TBABF_4$/DCM solution. All processes are reversible, unless otherwise stated; *irreversible.*

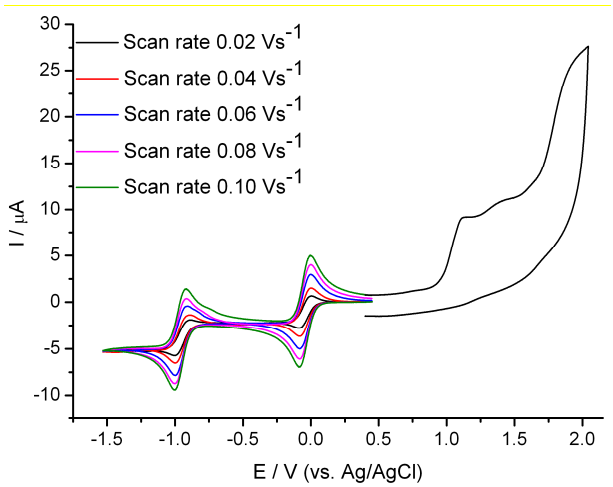

*Figure S3: Cyclic voltammetry of **4**, measuring current (I), in response to an applied potential (E), in 0.3 M $TBABF_4$/DCM.*

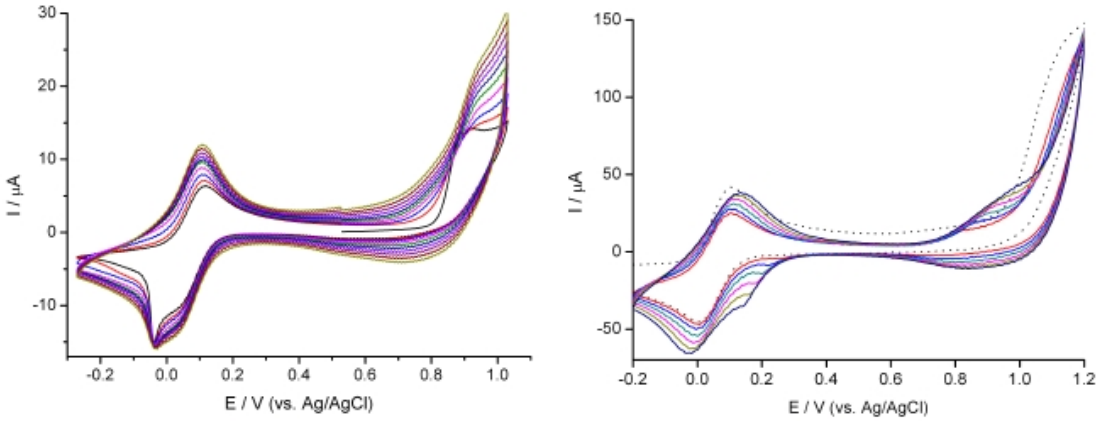

*Figure S4: Potential cycling into the first irreversible oxidation process to facilitate polymerisation (1 Vs^{-1}), measuring the current (I) response to a cycling potential (E): (left) a concentrated solution of **3** in 0.3 M $TBABF_4$/DCM, between -0.2 V and +1.1 V and (right) a concentrated solution of **4** in 0.1 M $TBABF_4$/MeCN, between -0.3 V and +1.2 V. Peak currents (\|Ip\|) increase with potential cycling, indicating the deposition of a conducting film.*

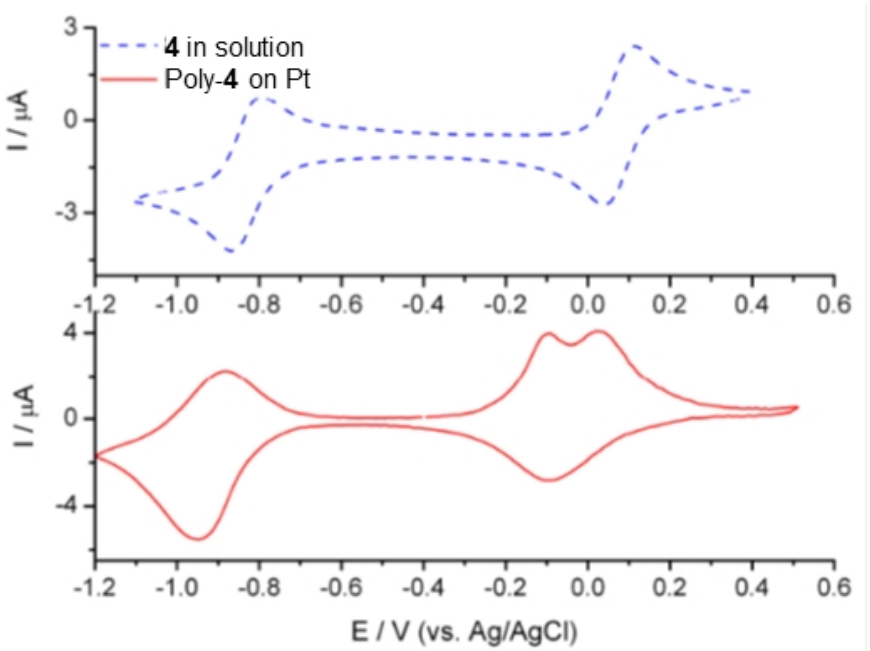

*Figure S5: Cyclic voltammetry of poly-**4** coated platinum electrode in monomer free electrolyte (0.3 M $TBABF_4$/MeCN) solution (lower), compared to the redox behaviour of the monomer in the same electrolyte system (upper).*

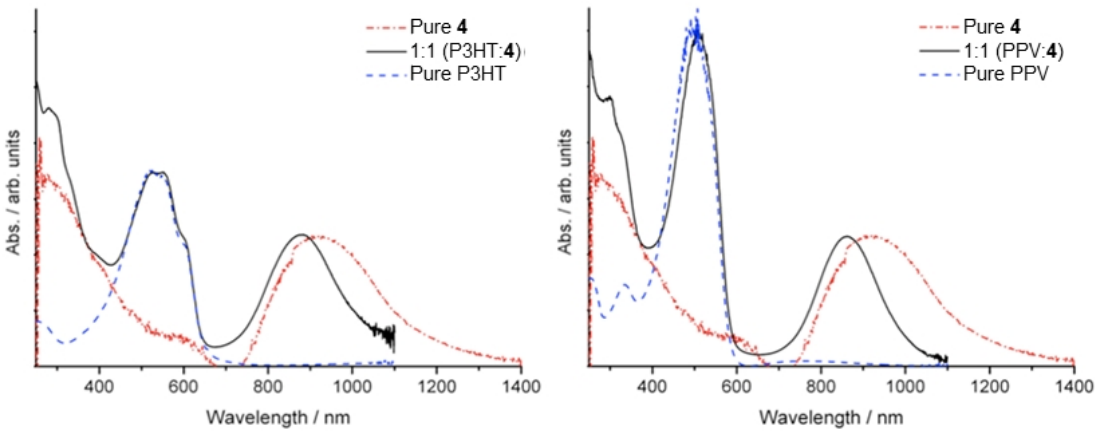

*Figure S6: UV/Vis absorbance spectra of spin coated films of, with the spectra of the pure films normalised with respect to the absorptions of the blend; (left) 1:1 P3HT:**4** blend, compared to pure P3HT and pure **4**; (right) 1:1 PPV:**4** blend, compared to pure PPV and pure **4***

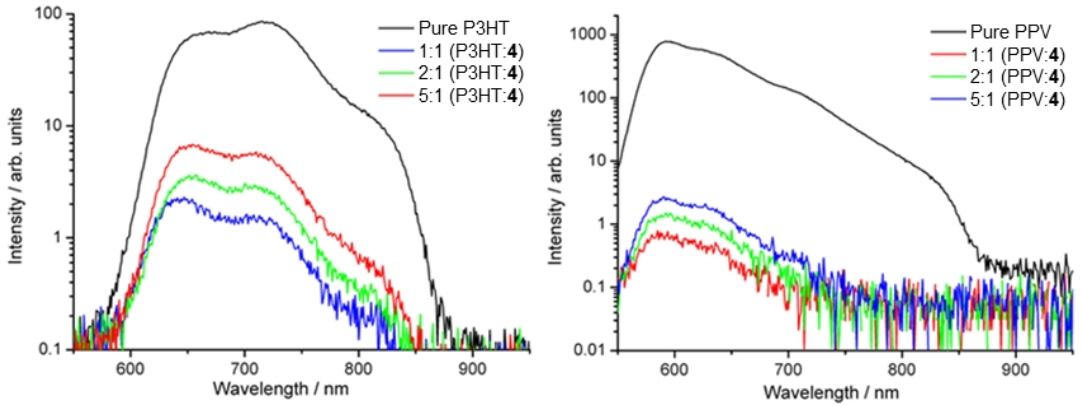

*Figure S7: Photoluminescence spectra of spin coated films of: (left) pure P3HT, compared to P3HT:**4** blends of weight ratios 1:1, 2:1 and 5:1; (right) pure PPV, compared to PPV:**4** blends of weight ratios 1:1, 2:1 and 5:1*